Proceedings of the
Annual Stability Conference
Structural Stability Research Council
Atlanta, Georgia, April 21-24, 2026

Strength and stability limits for stainless steel round HSS members under flexure

Guven Kiymaz[1], Marios K Chryssanthopoulos[2], Cumhur Cosgun[3]

Abstract

The release of AISC 370-21 introduced a dedicated U.S. design specification for structural stainless steel, offering updated provisions for the flexural design of round hollow structural sections (HSS). This study critically reassesses the cross-section slenderness limits specified in AISC 370-21 for round HSS members in flexure and compares them to those in the earlier SEI/ASCE 8-02 specification. The investigation draws upon a validated set of experimental and finite-element results for seam-welded stainless steel round HSS fabricated from both austenitic and duplex grades. These results reveal that many members exceeded both elastic and plastic moment capacities, even beyond the conservative slenderness thresholds permitted by ASCE 8-02. While AISC 370-21 reflects meaningful progress by introducing stainless-steel-specific classification rules, its current limits on section compactness and moment resistance still merit further evaluation. In addition, the Continuous Strength Method (CSM), provided in Appendix 2 of AISC 370-21, is employed to estimate the flexural strength of the tested members. This strain-based approach offers an alternative to traditional classification, accounting for material nonlinearity and deformation capacity. Moment strength predictions from the earlier ASCE 8-02, AISC 370-21, and the CSM are compared against test and simulation results to assess their relative accuracy and conservatism. The findings underscore the evolving treatment of stainless-steel round HSS in global design standards and identify areas for future refinement.

1. Introduction

Stainless steel circular hollow sections (CHS) or round hollow structural sections (round HSS) are increasingly utilized in structural applications due to their excellent corrosion resistance, durability, and aesthetic qualities. However, their flexural behavior exhibits distinct characteristics compared to that of conventional carbon-steel members, necessitating specialized investigation and design provisions. The nonlinear stress-strain relationship of stainless steel, characterized by gradual yielding and significant strain hardening, particularly in austenitic grades, fundamentally influences moment-rotation response and ultimate capacity (Rasmussen, 2003; Gardner, 2005). Comprehensive experimental programs have established that local buckling and cross-section slenderness are the governing factors in the flexural performance of round HSS (Theofanous &

[1] Assistant Professor, Florida Polytechnic University, gkiymaz@floridapoly.edu
[2] Professor, University of Surrey, mkchry@surrey.ac.uk
[3] Senior Civil Engineer, PennDOT, ccosgun@pa.gov

Gardner, 2009). Slender sections (high D/t ratios) typically fail through compression-side local buckling and ovalisation, while stocky sections develop full plastic moment capacity with substantial rotation capacity. Fabrication processes, particularly seam and girth welding, introduce residual stresses and geometric imperfections that promote premature local buckling and reduce both stiffness and ultimate strength (Rasmussen & Hancock, 1992; Cruise and Gardner, 2008).

Validated nonlinear finite element models have successfully replicated experimental behavior when incorporating measured material properties, initial imperfections, and weld residual stresses (Theofanous & Gardner, 2010; Afshan & Gardner, 2013). Comparative assessments reveal that current international design standards (Eurocode 3, AISC, AS/NZS) are generally conservative for stainless steel round HSS, suggesting potential for revised classification criteria and slenderness limits that capitalize on the material's superior ductility (Gardner et al., 2006; Theofanous & Gardner, 2009; Liew et al., 2010).

A major advancement in this direction is the recent publication of ANSI/AISC 370-21, which represents the first U.S. specification dedicated to structural stainless steel design. This standard incorporates stainless-steel-specific classification rules, strength formulations, and a new strain-based approach, the Continuous Strength Method (CSM), which is provided in its Appendix 2. A growing body of research has begun to assess and validate the provisions of AISC 370-21. Notably, studies have explored flexural buckling rules (Meza & Rossi, 2021), the use of second-order inelastic analysis (Walport et al., 2021), and reliability-based calibration of resistance factors (Gardner, 2024). Evaluations under cyclic loading and in the context of novel fabrication methods, such as wire arc additive manufacturing (WAAM), have also revealed areas where the current provisions may be overly conservative or incomplete (Huang et al., 2024; Chen et al., 2024; Arrais & Jandera, 2023).

Despite the progress made in AISC 370-21, there remains a need for further validation of its cross-section classification limits and moment strength provisions for round HSS in flexure. This study seeks to address this gap by reassessing existing experimental and numerical data on seam-welded stainless steel round HSS members and benchmarking their flexural performance against predictions from ASCE 8-02, AISC 370-21, and the Continuous Strength Method in Appendix 2 of the AISC 370-21.

2. Historical Development of Structural Stainless Steel Design Standards

Before presenting the methodology and results of this study, it is important to revisit the historical development of structural stainless steel design standards. Understanding how different standards have approached stainless steel over time highlights the evolution in design philosophy, from reliance on carbon steel to the adoption of material-specific models that reflect stainless steel's unique mechanical behavior. This context is essential not only for benchmarking the accuracy and conservatism of existing design provisions but also for identifying areas where further refinement may be needed. The comparative insights drawn from this historical background provide a foundation for evaluating the relevance and effectiveness of current code provisions, such as those in AISC 370-21.

The evolution of design standards for structural stainless steel has followed distinct trajectories across the United States, Europe, and Australia, each shaped by differing design philosophies, code traditions, and regional industry needs.

In the United States, early stainless steel design practice relied heavily on adaptations of carbon steel specifications, such as AISC 360, despite the significant differences in mechanical behavior between carbon and stainless steels—most notably, the absence of a distinct yield plateau, pronounced strain hardening, and rounded stress–strain curves in stainless steels. The first dedicated national design specification emerged with the publication of SEI/ASCE 8-02 in 2002, titled Specification for the Design of Cold-Formed Stainless Steel Structural Members. This standard, developed by the Structural Engineering Institute (SEI) of ASCE, addressed design rules for cold-formed stainless steel members in tension, compression, bending, and shear, but its scope was limited to members formed from sheet, strip, plate, and flat bar and it remained largely unmodified in the years following its release. SEI/ASCE 8-02 has recently been superseded by SEI/ASCE 8-22, which updates and extends the provisions for cold-formed stainless steel sections in line with more recent research and design methodologies. In parallel, the publication of ANSI/AISC 370-21, Specification for Structural Stainless Steel Buildings, in 2021 marked a significant advance by providing the first comprehensive U.S. specification for structural stainless steel building members. AISC 370-21 covers hot-rolled, welded, and cold-formed members, introduces stainless-specific cross-section classification and resistance factors, and incorporates the strain-based Continuous Strength Method (CSM) in Appendix 2. In this way, ASCE 8 and AISC 370-21 now serve complementary roles, with the former focused on cold-formed stainless steel sections and the latter providing a unified framework for structural stainless steel buildings.

In Europe, design guidance for structural stainless steel was initially provided through industry-led publications, most notably by Euro Inox in the early 2000s. Formal codification was achieved with the publication of EN 1993-1-4:2006, a part of the Eurocode 3 suite titled Design of Steel Structures – Part 1-4: Supplementary rules for stainless steels. This standard provided a comprehensive framework for the design of stainless steel members, including austenitic, ferritic, and duplex grades. It introduced material-specific stress–strain models, cross-section classification limits, and member strength formulations for tension, compression, bending, and shear. The standard was amended in 2015 (EN 1993-1-4:2006+A1:2015) to incorporate updates based on experimental evidence and evolving practice, and it remains the authoritative reference for structural stainless steel design across Europe, although a second-generation Eurocode is under development as part of the broader Eurocode revision process.

In Australia, design provisions were formalized with the publication of AS/NZS 4673:2001, titled Cold-Formed Stainless Steel Structures, developed jointly by Standards Australia and Standards New Zealand. This standard, modeled after AS/NZS 4600 for cold-formed carbon steel, adopted a limit-state design approach and provided rules for compression, bending, and shear behavior of cold-formed stainless steel members. While it acknowledged the distinctive material response of stainless steels, the design rules remained largely conservative. As of 2025, AS/NZS 4673 has not undergone a formal revision or update since its initial release, and no newer public edition has been identified. As a result, its design limits continue to reflect early-generation assumptions that predate more recent research findings and modeling approaches.

Taken together, the historical progression of stainless steel design standards illustrates the gradual shift from the adoption of carbon-steel rules to the development of dedicated, material-specific design methodologies. The publication of AISC 370-21 in the United States, together with ongoing updates to EN 1993-1-4 in Europe, marks a significant step toward harmonized, performance-based design for structural stainless steel worldwide, while the continued reliance on AS/NZS 4673 in Australia highlights the need for further modernization in some regions.

3. Experimental Study on Seam-Welded Round HSS Members

An experimental program was conducted to investigate the flexural behavior of seam-welded structural stainless steel round HSSs, with a particular focus on strength, deformation, and the influence of cross-section classification. The study involved eight full-scale round HSS specimens manufactured by roll-forming stainless steel strips and joining them with a continuous longitudinal seam weld. Two stainless steel grades were used: austenitic Grade 304 and duplex Grade 2205 (UNS S31803), each represented by four specimens. Tensile coupon tests were performed to characterize the material properties, using three 30 mm-wide longitudinal coupons extracted from each tube—one near the weld, one diametrically opposite, and one at 90 degrees to the weld. These tests confirmed the expected nonlinear stress-strain behavior of stainless steel, with no distinct yield plateau and considerable strain hardening (Fig.1). A consistent variation in 0.2% proof stress was observed, with the 90-degree locations tending to be weaker. Average values of the elastic modulus (E_0), 0.2% proof stress ($F_{0.2}$), and ultimate tensile strength (F_{max}) were subsequently used in design calculations and finite element modeling.

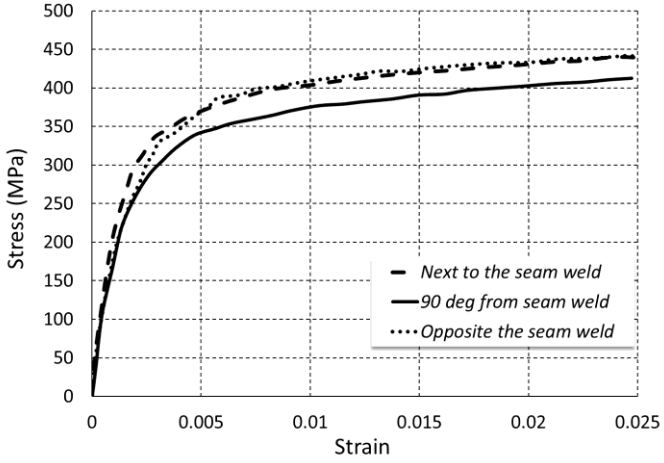

Figure 1: Stress-strain curves from tensile tests

The round HSS specimens were subjected to two-point bending tests under simply supported conditions. Tubes approximately 2 meters in length were fitted with four precision-machined steel ring collars at the supports and loading points. Load was applied incrementally through a spreader beam and cylindrical rollers, producing pure bending over a central region 500 mm in length. The support system used cylindrical rollers over lubricated Teflon plates to replicate simple support conditions. The seam weld in all specimens was placed at the top during testing, aligning with the compression zone to promote symmetry and maximize sensitivity to local buckling. Displacement transducers were positioned at the load points and at midspan to measure vertical deflection. A separate gauge with length $4\sqrt{Dt}$ was used to measure initial geometric imperfections along the tube length. With the exception of specimen TB07, which had a non-ground weld, initial

imperfections were found to be minimal. The experimental program confirmed that fabrication processes—particularly seam welding—introduced minor geometric irregularities and residual stress patterns, but the dominant factors influencing flexural capacity were cross-section slenderness and material nonlinearity. The resulting dataset was critical for validating finite element models and assessing the conservatism of existing design specifications.

4. Finite-Element Analysis of Stainless-Steel Round HSS Members

4.1 General Approach to FE Analysis

Numerical modeling of stainless steel round HSS members was conducted utilizing ABAQUS, a versatile finite-element program capable of handling both linear and complex nonlinear analyses, including those involving manufacturing distortions and material nonlinearities. The initial phase of analysis focused on simulating the experimental study of eight stainless steel round HSS members subjected to two-point bending. Following successful validation of these experimental tests through FE modeling, a parametric study was undertaken to generate additional results across a practical range of cross-sectional slenderness values.

4.2 ABAQUS Round HSS Model Details

The finite element models for the stainless steel round HSS members were developed in ABAQUS using four-node doubly curved shell elements (S4R), which are well-suited for capturing the complex deformation behavior of thin-walled tubular structures. Particular attention was given to mesh refinement in regions expected to experience local buckling and in areas influenced by welding-induced residual stresses. A denser mesh was applied to the upper half of each tube model to align with the assumed distribution of residual stresses and to improve accuracy in the compression zone. The central span, where local instability was anticipated, also used a finer mesh to capture localized deformation and failure modes accurately (Fig. 2).

To replicate the experimental setup, rigid ring collars were modeled at the load application points using ABAQUS's analytical rigid shell elements. These collars were treated as rigid bodies, appropriate for simulating stiff components where internal stress distributions are not of primary interest. Each collar was associated with a reference node at its centroid, which possessed all six degrees of freedom (Fig.2). Loads were applied as concentrated forces to these reference nodes. The interaction between the rigid collars and the outer surfaces of the round HSS members was modeled using surface-based contact with a finite-sliding formulation, enabling a realistic simulation of load transfer and boundary effects.

Boundary conditions were implemented to reproduce the simply supported end restraints observed in testing. Nodes at each tube end were permitted to translate axially and rotate about the transverse axis, while being restrained in lateral translation and other rotational degrees of freedom to prevent rigid-body displacement. This setup ensured that the model behavior remained consistent with the experimental conditions.

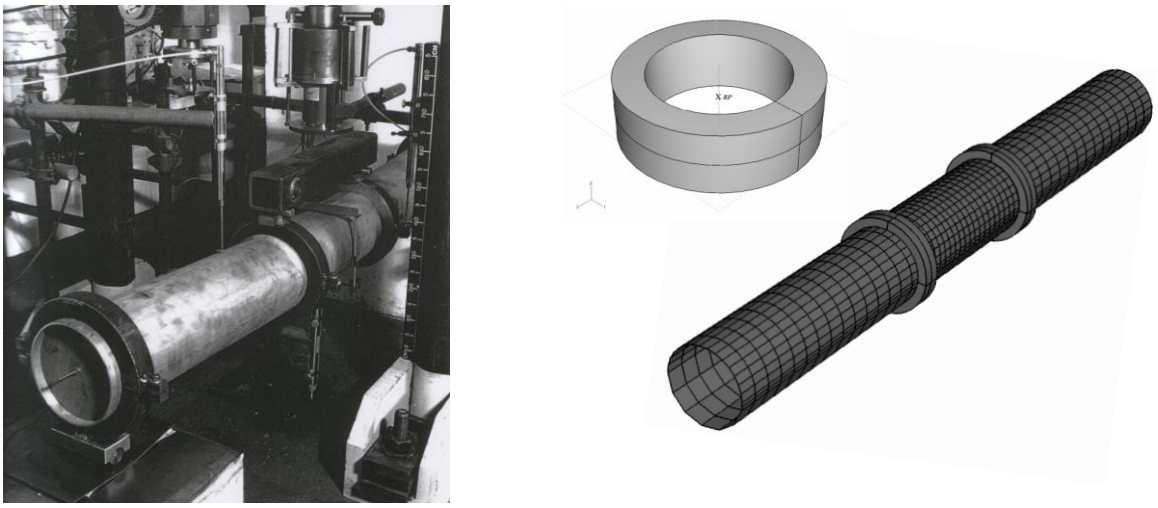

Figure 2: Experimental setup and corresponding FE model

Material behavior was captured using a nonlinear stress-strain input derived from experimental tensile test results. Rather than employing an idealized elastic–perfectly plastic material model, true stress–plastic strain data were input directly into ABAQUS, based on the average of three tensile coupons sampled from each tube at multiple orientations. A constant Poisson's ratio of 0.3 and elastic modulus values taken from coupon test data were used in all models.

Residual stresses introduced by seam welding were incorporated using a simplified residual stress block model adapted from Gao et al. (1998). The stress pattern, applied via ABAQUS's initial conditions functionality, introduced tensile stresses along the weld line and compensating compressive stresses on adjacent surfaces (Fig.3). A preliminary analysis step was conducted to equilibrate these residual stresses prior to applying external loading. Although originally developed for carbon steel, the stress block model was considered a practical approximation in the absence of detailed residual stress distributions for seam-welded stainless steel round HSS members.

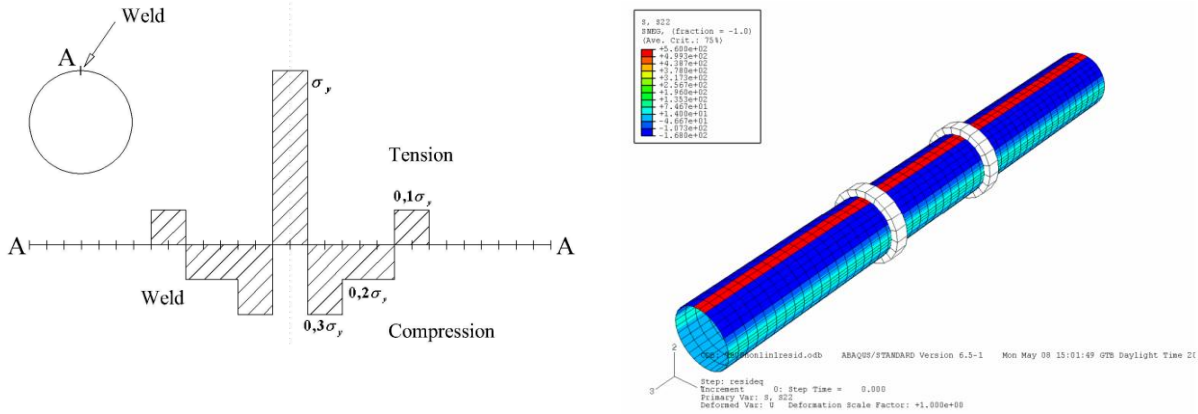

Figure 3: Weld-induced residual stress-block model proposed by Gao et al. (1998)

The finite element analysis aimed to accurately predict the behavior of stainless steel round HSS members under bending, incorporating material nonlinearity, manufacturing distortions, and appropriate boundary conditions. The models were designed to capture both the overall load-deformation response and specific failure modes, such as local buckling, providing a robust basis for evaluating design recommendations.

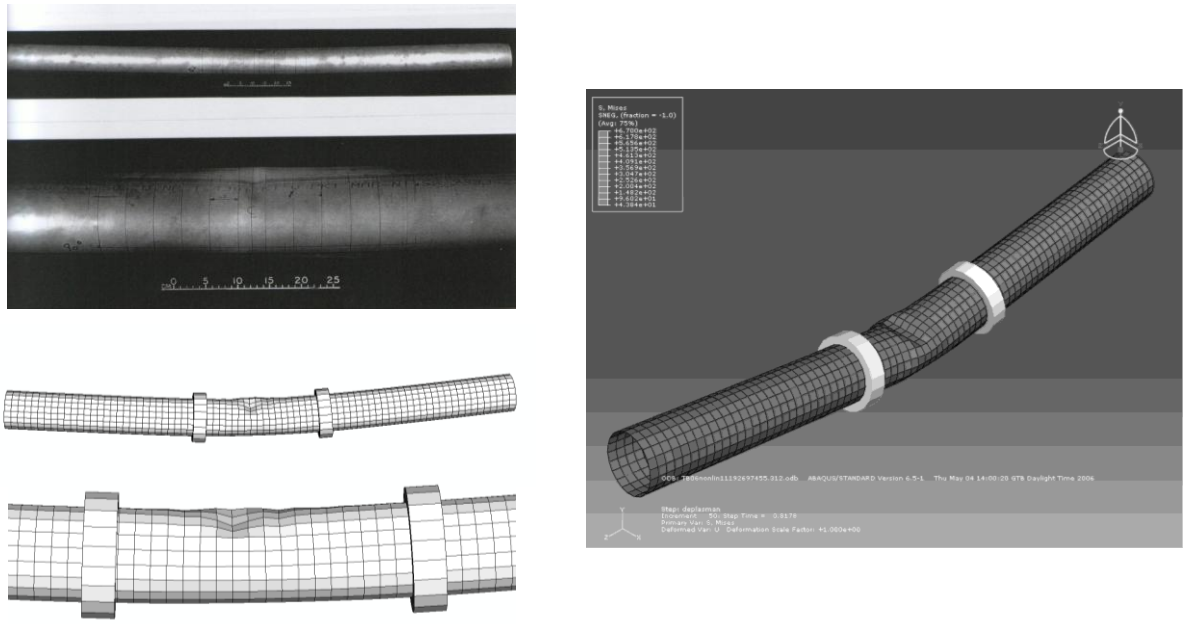

Figure 4: Local buckling captured using the FE model

4.3 Nonlinear Finite-Element Analysis

Nonlinear finite element analysis was employed to investigate the flexural behavior and ultimate strength of stainless steel round HSS members. Simulations were carried out using ABAQUS, which solves the nonlinear equilibrium equations using an incremental-iterative procedure based on the Newton–Raphson method. In this approach, the applied load is divided into a series of increments, and equilibrium is iteratively enforced at each step until convergence is achieved. This method enables the capture of complex material and geometric nonlinearities inherent in stainless steel members, particularly under large deformation and post-buckling conditions.

Nonlinear static analyses were performed on the tested round HSS specimens to validate the models' accuracy by comparing simulation results with experimental observations. Once validated, the models were also extended into a broader parametric study, allowing exploration of a wider range of diameter-to-thickness ratios and geometric configurations beyond the test matrix.

Load-displacement responses were extracted from the models using defined output variables (Fig. 5). The applied loads were recorded at the reference nodes associated with the rigid ring collars, where point loads were applied. Corresponding vertical displacements were obtained from a node located at the mid-span of the tube, directly beneath the neutral axis, mimicking the position of the central transducer used in physical testing to measure vertical deflection. This alignment enabled

a consistent and direct comparison between finite element results and experimental load-displacement curves.

Table 1 compares the ultimate moments of the tubes from the tests with those predicted by FE modeling. Using the finite-element modeling assumptions mentioned earlier, FE predictions of key performance measures, such as the load-deformation response and ultimate strength, closely align with the test results.

Overall, the nonlinear finite element analysis established a solid numerical foundation for simulating the flexural behavior of stainless steel round HSS members. The models were validated through precise data extraction and correlation with test results, boosting confidence in their use for assessing the relevance of design provisions, such as those in AISC 370-21 and the Continuous Strength Method.

Table 1: Comparison of Test and Finite Element Ultimate Moments
for Seam-Welded Stainless Steel round HSS Members

RHSS specimen identification	RHSS slenderness $(E_0/F_\gamma)/(D/t)$	Test ultimate moment (M_u Test)	FE ultimate moment (M_u FE)	$M_{u,\ Test}$ / $M_{u,\ FE}$
TB01	5.78	6.53	7.06	0.92
TB02	3.72	13.69	14.44	0.95
TB03	3.68	17.7	18.43	0.96
TB04	4.9	28.01	29.1	0.96
TB05	7.3	21.98	23.4	0.94
TB06	6.67	61.23	60.75	1.01
TB07	4.57	62.63	71.63	0.87
TB08	6.17	102	108.75	0.94
Mean				0.944
Standard deviation				0.04

4.4 Parametric Study

Following the close agreement between the experimental results and the finite element (FE) simulations, a broader parametric investigation was undertaken to expand the database and support a more general evaluation of design provisions for stainless steel round HSS members in bending. The validated FE model was used as a template, and a reference tube corresponding to test specimen TB06 was adopted, keeping the round HSS diameter and material properties constant. Variations in cross-section slenderness were then introduced by modifying only the wall thickness.

Table 2 summarizes the additional FE models considered. The resulting set of tubes spans a generalized slenderness range of approximately $2.5 \le (E_0/F_y)/(D/t) \le 12$, or $0.08\ E_0/F_y \le D/t \le 0.4\ E_0/F_y$, which corresponds to the practical spectrum in which members are expected to fail either by elastoplastic local buckling or by yielding. Ultimate moment capacities predicted by ABAQUS for these models, together with the test results from the physical specimens, form the dataset used in subsequent sections to appraise the adequacy and conservatism of current design recommendations for stainless steel round HSS members.

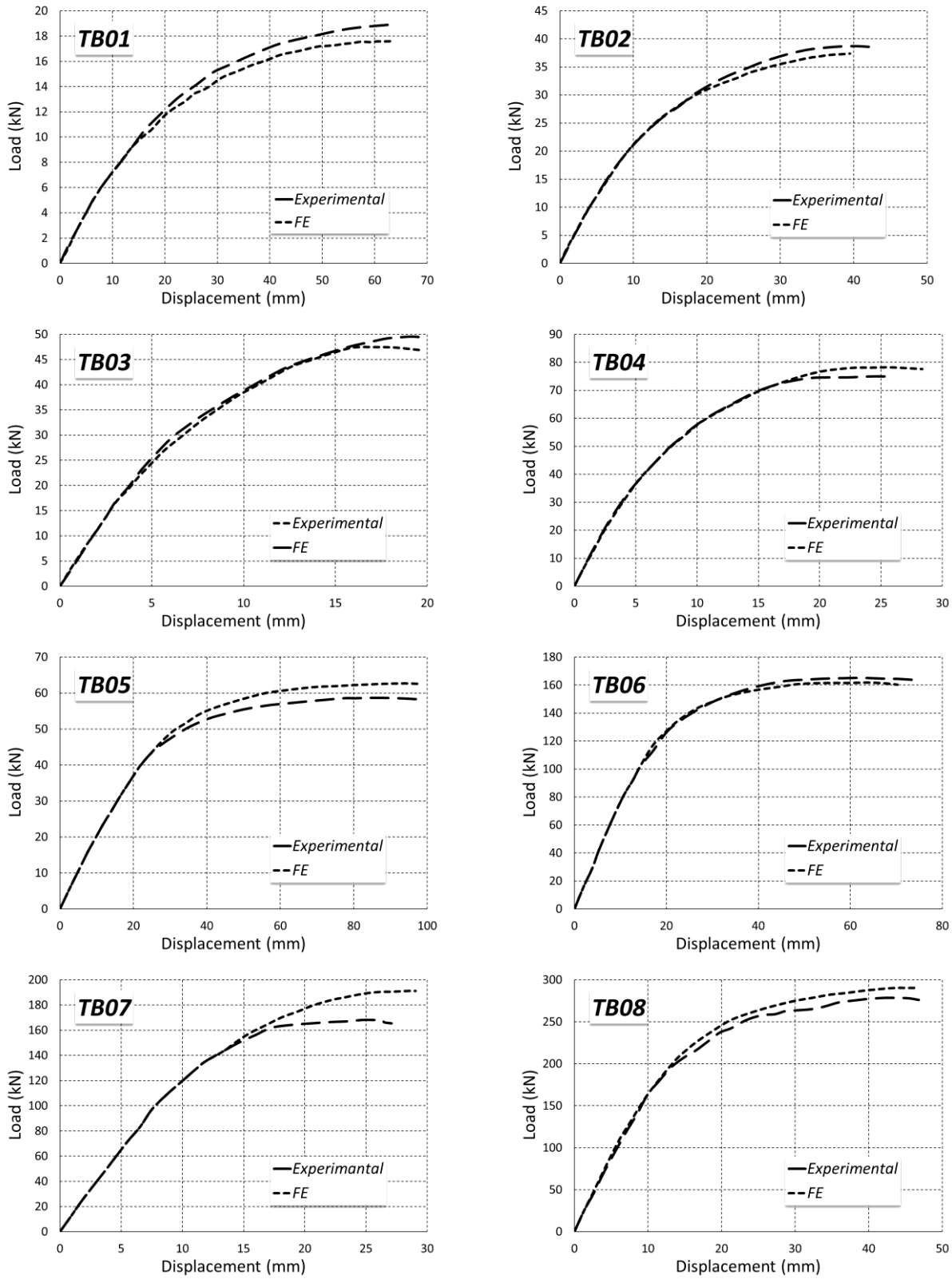

Figure 5: Load-displacement response curves (Experimental and FE)

Table 2: Summary of Additional Parametric FE Models with Varying Slenderness

FE model identification	Tube slenderness $(E_o/F_y)/(D/t)$	Thickness (mm)
TB09	2.5	1.27
TB10	3	1.52
TB11	7.5	3.8
TB12	8	4.05
TB13	8.5	4.31
TB14	9	4.56
TB15	9.5	4.81
TB16	10	5.07
TB17	10.5	5.32
TB18	11	5.57
TB19	12	6.08

Note: CHS Diameter = 168.3 mm (constant); Material: Same as assumed for TB06 (168.3 x 3.40).

5. Overview of Design Provisions

5.1 Flexural Strength based on SEI-ASCE 8 – (2002)

In the SEI/ASCE 8-02 Specification, the flexural strength of stainless steel round HSS members is governed entirely by elastic behavior; plastic moment resistance is not permitted for these sections. For members under bending, the specification first limits the use of the elastic moment resistance,

$$M_n = F_y S_f \tag{1}$$

to relatively stocky tubes with

$$\frac{D}{t} \leq 0.112 \frac{E_0}{F_y} \tag{2}$$

expressed in terms of the generalized slenderness parameter $(E_0/F_y)/(D/t)$. For more slender round HSS with

$$0.112 \frac{E_0}{F_y} < \frac{D}{t} \leq 0.881 \frac{E_0}{F_y} \tag{3}$$

the nominal moment is reduced by a nonlinear factor K_c so that

$$M_n = K_c F_y S_f \tag{4}$$

The reduction factor K_c is defined as

$$K_c = \frac{(1-C)(E_0/F_y)}{(8.93-\lambda_c)(D/t)} + \frac{5.882\,C}{8.93-\lambda_c} \tag{5}$$

where C is the ratio of effective proportional limit to yield strength and $\lambda_c = 3.048C$ is a limiting value of $(E_0/F_y)/(D/t)$ associated with elastic local buckling of slender round HSS members. Values of C are provided in ASCE 8-02 Table A17 for different stainless steel grades and typically range from about 0.29 to 0.83; lower values of C *lead* to smaller K_c and hence more conservative

moment resistances. In this study, strength calculations according to the ASCE 8-02 specification were carried out, assuming $C = 0.83$ for all of the specimens, so that the predicted strengths represent the upper bound associated with the highest proportional-limit–to–yield ratio given in the specification. If $C = 1.0$, the reduction factor becomes $K_c = 1.0$ and the expression reduces to simple elastic moment capacity. The specification does not provide explicit guidance for members with $D/t > 0.881\, E_0/F_y$, so very slender CHS sections fall outside the recommended limits for flexural design.

5.2 Flexural Strength based on ANSI-AISC 370 – 2021

In AISC 370-21, the flexural design of stainless steel round HSS is treated in Section F8. The provisions apply to compact and noncompact round HSS, with cross-section classification based on the diameter-to-thickness ratio $\frac{D}{t}$ given in Table B4.1b. A member is classified as compact if

$$\frac{D}{t} \leq \lambda_p = 0.08\, \frac{E_0}{F_y} \tag{6}$$

and as noncompact if

$$\lambda_p < \frac{D}{t} \leq \lambda_r = 0.31\, \frac{E_0}{F_y} \tag{7}$$

where E_0 is the modulus of elasticity, and F_y is the specified minimum yield stress. Members with $\frac{D}{t} > \lambda_r$ are classified as slender. Chapter F does not provide a closed-form flexural resistance expression for these slender round HSS; instead, the Commentary notes that such members may be designed using the Continuous Strength Method (CSM) in Appendix 2, provided that,

$$\frac{D}{t} \leq 0.44\, \frac{E_0}{F_y} (\text{or } \lambda_l \leq 0.60) \tag{8}$$

so that the strain-based CSM formulation governs their moment capacity.

For compact and noncompact round HSS, the nominal flexural strength M_n is taken as the lower of the strengths corresponding to yielding (plastic moment) and local buckling. The yielding limit state is

$$M_n = M_p = F_y Z \tag{9}$$

where $Z$is the plastic section modulus. Local buckling affects only noncompact sections, for which the nominal moment is reduced according to

$$M_n = \left(\frac{0.068\, \lambda_r}{\lambda} + 1\right) F_y S \tag{10}$$

with $\lambda = \frac{D}{t}$ and S the elastic section modulus. Thus, compact round HSS are permitted to reach the full plastic moment, noncompact sections have an interpolated capacity between elastic and plastic limits as a function of $\frac{D}{t}$, and slender sections within the specified upper bound on $\frac{D}{t}$ are to be designed using the CSM rather than the traditional classification-based expressions.

5.3 The Continuous Strength Method (CSM) (ANSI-AISC 370, Appendix 2)

The Continuous Strength Method (CSM) in Appendix 2 of AISC 370-21 is a deformation-based design approach that exploits the strain-hardening capacity of stainless steel and the beneficial interaction of elements within the cross-section. It applies to round HSS subjected to bending and combined loading. For round HSS, the CSM characterizes cross-section behavior through a "full cross-section slenderness" parameter, λ_l, and a corresponding deformation capacity expressed as a strain ratio $\frac{\varepsilon_{csm}}{\varepsilon_y}$. Regression-based base curves relate $\frac{\varepsilon_{csm}}{\varepsilon_y}$ to λ_l; for nonslender round HSS ($\lambda_l \leq 0.30$) the strain ratio is greater than or equal to unity, allowing the method to utilize strain hardening, whereas for slender sections ($\lambda_l > 0.30$) the strain ratio is less than unity and local buckling limits the attainable strain.

Once ε_{csm} is established, the flexural design stress distribution is derived from an elastic, linear-hardening material model calibrated for austenitic and duplex stainless steels. For slender round HSS in bending about an axis of symmetry, the CSM nominal moment is obtained as the elastic bending resistance multiplied by the strain ratio $\frac{\varepsilon_{csm}}{\varepsilon_y}$, so no additional benefit from strain hardening is taken. For nonslender round HSS, an analytical integration of the CSM stress block leads to a simplified design expression in which the nominal moment is amplified above the elastic (and, for very stocky sections, above the conventional plastic) resistance through a CSM bending coefficient, α, that depends on cross-section shape and bending axis. In this way, the CSM provides a continuous, strain-based prediction of flexural strength for stainless steel round HSS, bridging the gap between elastic, yield-based design and the actual strain-hardening response observed in tests.

Table 3: Cross Section Slenderness (D/t) Limits for Stainless Steel round HSS Flexural Members

Design standards	D/t slenderness limit for plastic moment resistance	D/t slenderness limit for elastic moment resistance	Greater slenderness values
SEI/ASCE 8-02 (2002)	No guidance	0.112 E_0/F_y	Up to 0.881E_0/F_y
ANSI/AISC 370-21	0.08 E_0/F_y	0.31 E_0/F_y	Use CSM in Appendix 2*
EN 1993-1-4	0.078 E_0/F_y	0.313 E_0/F_y	No guidance
AS/NZS 4673 (2001)	0.078 E_0/F_y	0.313 E_0/F_y	Up to 0.881E_0/F_y

*For slenderness values greater than 0.31 E_0/F_y, use the Continuous Strength Method in Appendix 2, provided D/t < 0.44 E_0/F_y

A comparison of the specifications regarding limiting slenderness values for design bending moment resistance calculations is presented in Table 3. This table highlights several important differences in how the various standards treat stainless steel round HSS in flexure. SEI/ASCE 8-02 does not permit plastic moment resistance for CHS members and restricts the use of the elastic moment to relatively stocky tubes with $D/t \leq 0.112\, E_0/F_y$; for more slender sections, the specification relies on a reduction factor up to an upper limit of $D/t = 0.881\, E_0/F_y$. In contrast, AISC 370-21, EN 1993-1-4, and AS/NZS 4673 all provide explicit slenderness limits for plastic moment resistance, with closely aligned thresholds of approximately 0.078–$0.08\, E_0/F_y$, and higher limits for elastic moment resistance of about 0.31–$0.313\, E_0/F_y$. Beyond the elastic limit, EN 1993-1-4 offers no specific guidance, whereas AS/NZS 4673, similar to ASCE 8-02, gives an

upper bound of $0.881\ E_0/F_y$ for very slender members. AISC 370-21 differs from both approaches by directing designers to the Continuous Strength Method in Appendix 2 for round HSS with $D/t > 0.31\ E_0/F_y$ (provided $D/t < 0.44\ E_0/F_y$), thereby replacing discrete classification limits with a strain-based formulation that can exploit deformation capacity in the intermediate-to-slender range.

6. Evaluation of Design Provisions Based on Test and FE Results

The comparison of test and code-based moment predictions in Fig. 6 reveals several important trends. When plotted as the ratio of moment to elastic moment against the generalized tube slenderness $(E_0/F_y)/(D/t)$, with lower values on the left corresponding to more slender members and higher values on the right corresponding to stockier members, the experimental and FE results demonstrate that stainless steel round HSS possess significant flexural reserve beyond the elastic limit.

For relatively slender tubes (left side of the plot), the test points cluster slightly above the elastic moment line, indicating that even these members can at least attain, and often modestly exceed, the elastic resistance. As the sections become stockier (moving to the right), the test ratios increase steadily and many values approach or exceed the conventional plastic moment level, highlighting the pronounced strain-hardening capacity of the material.

The ASCE 8-02 predictions lie consistently below the experimental results over the full slenderness range. For slender members, the specification typically predicts only about 0.8–0.9 of the elastic moment, and it remains conservative even for stockier tubes within its prescribed range of applicability. In contrast, the AISC 370-21 Chapter F provisions for round HSS (Section F8) provide a much closer approximation to the observed behavior. The F8 nominal moments generally track the test data well, lying just below the experimental points for both slender and stocky members and reproducing the increasing strength trend as slenderness decreases.

The Continuous Strength Method (CSM) of Appendix 2 exhibits an intermediate level of conservatism. For slender members, the CSM predictions are similar to those from ASCE 8-02 and therefore noticeably below the tests. However, as the sections become stockier—beyond the ASCE limit for elastic moment resistance—the CSM strengths increase approximately linearly with decreasing slenderness and progressively converge toward the F8 predictions and the experimental results.

Overall, the figure indicates that Section F8 of AISC 370-21 currently offers the best agreement with measured flexural strengths of stainless steel round HSS, while the CSM provides a rational, strain-based alternative that remains conservative relative to F8 but represents a substantial improvement over ASCE 8-02, particularly for stockier sections.

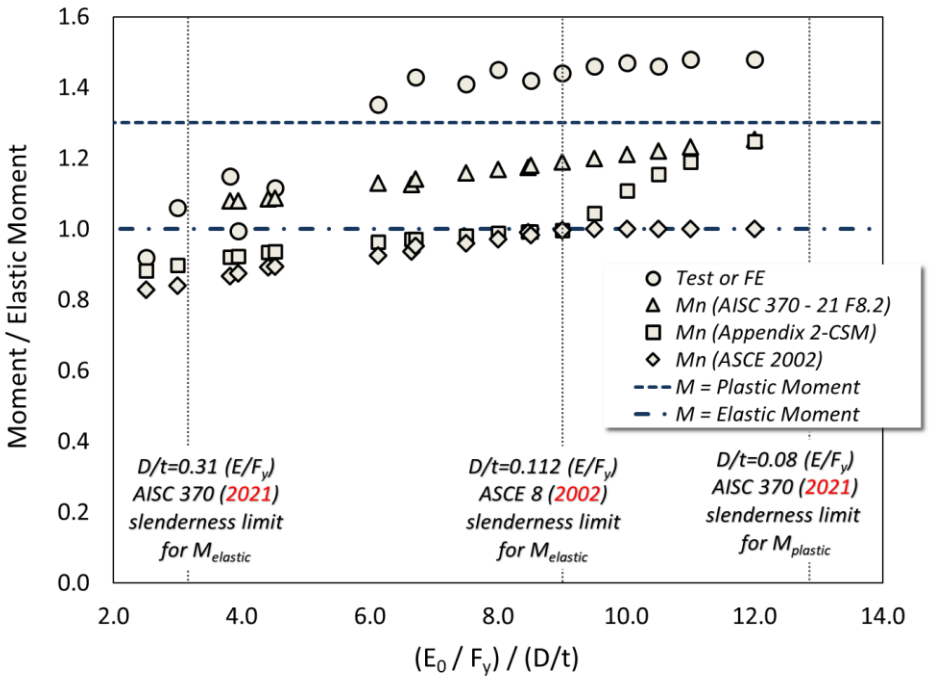

Figure 6: Comparison of test and code-based moment predictions

7. Conclusions

An experimental and numerical study on seam-welded stainless steel round HSS under pure bending has been used to evaluate the accuracy and conservatism of three design approaches for stainless steel round HSS in flexure: the SEI/ASCE 8-02 specification, the AISC 370-21 provisions in Section F8, and the Continuous Strength Method (CSM) in Appendix 2 of AISC 370-21. Based on the comparisons between test/FE results and code predictions over a wide range of cross-section slenderness, the following conclusions may be drawn:

- The test and finite-element results confirm that stainless steel round HSS members exhibit significant flexural reserve beyond the elastic moment, particularly for stocky sections. Even relatively slender sections were generally able to achieve at least the elastic moment, while stockier sections frequently reached or exceeded the conventional plastic moment resistance.
- The SEI/ASCE 8-02 specification was found to be consistently conservative across the full range of slenderness considered. Its predictions typically underestimated the experimental moment capacities by 10–25%, and the slenderness limit for elastic moment resistance appears restrictive when measured against the demonstrated performance of the tested members.
- The AISC 370-21 flexural provisions for round HSS in Section F8 provided the closest overall agreement with the experimental and FE data. The F8 nominal strengths tracked the measured moment capacities well for both slender and stocky tubes, reproducing the observed trend of increasing strength with decreasing slenderness and making more effective use of the strain-hardening capacity of stainless steel than ASCE 8-02.

- The Continuous Strength Method in Appendix 2 of AISC 370-21 produced predictions that were generally conservative relative to both the test results and the F8 provisions. For slender sections, CSM strengths were similar to those given by ASCE 8-02, but for stockier sections, the CSM predictions increased almost linearly with decreasing slenderness and converged toward the F8 values, representing a substantial improvement over ASCE 8-02 while retaining a moderate safety margin.
- Although SEI/ASCE 8-02 has recently been superseded by SEI/ASCE 8-22, the comparisons presented in this study are intentionally limited to the provisions of SEI/ASCE 8-02. The bending strengths predicted by SEI/ASCE 8-02 are evaluated against a set of test and finite-element results for stainless steel round HSS members, and these predictions are used primarily as a benchmark for assessing the newer ANSI/AISC 370-21 provisions, including both the Section F8 rules and the Continuous Strength Method in Appendix 2. The major focus of the paper is therefore on examining the performance, accuracy, and conservatism of AISC 370-21 in light of these test and numerical results and in comparison with the legacy SEI/ASCE 8-02 specification. A detailed quantitative evaluation of the updated SEI/ASCE 8-22 specification is beyond the scope of the present work and is identified as a topic for future study.
- The results indicate that the current AISC 370-21 treatment of stainless steel round HSS in Section F8 is broadly appropriate and well calibrated for the range of specimens considered. At the same time, the comparisons suggest that some relaxation of cross-section slenderness limits could be explored in future specification developments, particularly in light of the demonstrated ability of noncompact sections to reach or exceed the elastic moment.
- The study also shows that the CSM offers a rational, deformation-based framework that can complement traditional classification-based design. Although conservative in its present form for round HSS, the method has the potential to underpin future refinements of slenderness limits and resistance factors once additional experimental data for stainless steel round HSS in flexure become available.
- Overall, the findings support the continued use of AISC 370-21 Section F8 for the design of stainless steel round HSS in bending and point to the CSM as a promising avenue for future code refinement.

References

AISC (2021). Specification for Structural Stainless Steel Buildings (ANSI/AISC 370-21). American Institute of Steel Construction, Chicago, IL.

ASCE (2002). Specification for the Design of Cold-Formed Stainless Steel Structural Members (SEI/ASCE 8-02). Structural Engineering Institute of the American Society of Civil Engineers, Reston, VA.

CEN (2015). Eurocode 3: Design of Steel Structures – Part 1-4: General Rules – Supplementary Rules for Stainless Steels (EN 1993-1-4:2006 + A1:2015). European Committee for Standardization (CEN), Brussels, Belgium.

Standards Australia/Standards New Zealand (2001). Cold-Formed Stainless Steel Structures (AS/NZS 4673:2001). Sydney, Australia / Wellington, New Zealand.

Afshan, S., & Gardner, L. (2013). The continuous strength method for structural stainless steel design. Thin-Walled Structures, 68, 42–49.

Arrais, F., & Jandera, M. (2023). Application limits of the general method for beam-columns in AISC 370-21. Journal of Constructional Steel Research, 205, 107812.

Chen, Y., Wang, Y., & Gardner, L. (2024). Section classification under cyclic loading for stainless steel structures. Engineering Structures, 302, 115952.

Cruise, R. B., & Gardner, L. (2008). Residual stress distributions and their influence on structural performance of stainless steel sections. Journal of Constructional Steel Research, 64(3), 352–362.
Gardner, L. (2005). A new approach to stainless steel design. Structural Engineer, 83(21), 28–33.
Gardner, L. (2024). Development of resistance factors for stainless steel design in U.S. specifications. Journal of Structural Engineering, in press.
Gardner, L., Afshan, S., & Theofanous, M. (2006). Behaviour of stainless steel members and comparison with carbon steel design. Thin-Walled Structures, 44(5), 517–527.
Gao, S., Usami, T., & Ge, H. (1998). Ductility of steel short cylinders in compression and bending. Journal of Engineering Mechanics, 124(2), 176–183.
Huang, Y., Wang, Z., & Feng, R. (2024). Flexural and compressive behavior of WAAM stainless steel tubular sections. Additive Manufacturing, 65, 102962.
Liew, J. Y. R., Shanmugam, N. E., & Teo, M. H. (2010). Thin-walled structures in steel construction: advances and challenges. Thin-Walled Structures, 48(12), 877–886.
Meza, D. C., & Rossi, B. (2021). Flexural buckling design of stainless steel members in the AISC 370-21 Specification. Proceedings of the SSRC Annual Stability Conference.
Rasmussen, K. J. R. (2003). Full-range stress-strain curves for stainless steel alloys. Journal of Constructional Steel Research, 59(1), 47–61.
Rasmussen, K. J. R., & Hancock, G. J. (1992). Design of cold-formed stainless steel tubular members. Journal of Structural Engineering, 118(5), 1269–1285.
Theofanous, M., & Gardner, L. (2009). Testing and numerical modelling of lean duplex stainless steel CHS beam-columns. Engineering Structures, 31(12), 3047–3058.
Theofanous, M., & Gardner, L. (2010). Finite element modelling of structural stainless steel cross-sections. Thin-Walled Structures, 48(7), 747–760.
Walport, L. J., Gardner, L., & Yuan, H. (2021). Second-order inelastic analysis for stainless steel frames: A CSM-based design approach. Journal of Structural Engineering, 147(11), 04021167.